



OPEN ACCESS

EDITED BY

Hu Li,
Sichuan University of Science and
Engineering, China

REVIEWED BY

Yuqiang Jiang,
Southwest Petroleum University, China
Siyi Fu,
Chengdu University of Technology, China

*CORRESPONDENCE

Jianhai Li,
✉ 13547835586@163.com

RECEIVED 02 March 2025

ACCEPTED 25 April 2025

PUBLISHED 09 May 2025

CITATION

Cen Y, Li J, Liang F, Wang L and Zhang X
(2025) Strike-slip fault system and its control
on ediacaran hydrocarbon system in central
Sichuan Basin: insights from petrology, U-Pb
dating and seismic interpretation.
Front. Earth Sci. 13:1586132.
doi: 10.3389/feart.2025.1586132

COPYRIGHT

© 2025 Cen, Li, Liang, Wang and Zhang. This
is an open-access article distributed under
the terms of the [Creative Commons
Attribution License \(CC BY\)](https://creativecommons.org/licenses/by/4.0/). The use,
distribution or reproduction in other forums is
permitted, provided the original author(s) and
the copyright owner(s) are credited and that
the original publication in this journal is cited,
in accordance with accepted academic
practice. No use, distribution or reproduction
is permitted which does not comply with
these terms.

Strike-slip fault system and its control on ediacaran hydrocarbon system in central Sichuan Basin: insights from petrology, U-Pb dating and seismic interpretation

Yongjing Cen¹, Jianhai Li^{2*}, Feng Liang¹, Lien Wang¹ and Xin Zhang²

¹North Central Sichuan Gas Production Management Office, PetroChina Southwest Oil and Gas Field Company, Suining, China, ²Fores (Chengdu) Technology Co., Ltd., Chengdu, China

Strike-slip faults are closely related to the enrichment of hydrocarbon resources, with a series of large oil and gas fields associated with strike-slip faults discovered in regions such as the Ordos Basin in China and the West Siberian Basin. The Ediacaran hydrocarbon resources in the Sichuan Basin are abundant. Identifying strike-slip faults and understanding their control over hydrocarbon systems is crucial for expanding exploration efforts. Based on lithology, seismic interpretation, and absolute age data, the strike-slip faults in the Ediacaran system and the overlying strata have been identified and classified. The patterns and evolutionary processes of strike-slip faults have been revealed. The results indicate that the planar patterns of strike-slip faults can be classified into linear, en echelon, and oblique structures. Strike-slip faults are typically seen as vertical (or steep) linear faults or flower-shaped structures in seismic profiles. Vertical (or steep) linear faults can further be categorized into transtensional high-steep structures and transpressional high-steep structures. The evolution of strike-slip faulting in the Central Sichuan Basin can be divided into four distinct stages: (1) a rifting stage during the Cryogenian, (2) a dextral transtensional strike-slip stage from the late Ediacaran to early Cambrian, (3) a dextral, weak transpressional strike-slip stage from the early Ordovician to early Permian, and (4) a sinistral transtensional strike-slip stage during the late Permian to early Triassic. The aulacogen, formed during the Cryogenian, controlled the distribution of the mound-shoal complex of the Dengying Formation and the thickness zones of the Cambrian hydrocarbon source rocks. The strike-slip faults in the first stage facilitated direct lateral and vertical contact between the overlying hydrocarbon source rocks and reservoirs, significantly enhancing the migration and accumulation efficiency of hydrocarbons. The strike-slip faults in the second stage controlled the distribution of ancient sedimentary paleogeomorphology and favorable karst

locations. The strike-slip faults in the third stage governed the distribution of gas and water.

KEYWORDS

strike-slip fault, ediacaran, seismic interpretation, hydrocarbon system, controlling effect

Introduction

The study of Structurally controlled hydrothermal fluid alteration mechanisms in reservoirs has become a key focus in the field of petroleum and natural gas geology (Hu et al., 2018; Koeshidayatullah et al., 2020). Starting in the 1980 s, North America pioneered research on hydrothermal reservoir formation in carbonate rocks influenced by deep large faults (Hurley and Swager, 1989). This concept later became recognized as a significant mechanism of reservoir formation in carbonates, leading to a re-evaluation of carbonate reservoir development models in many oil and gas basins worldwide (Davies and Smith Jr, 2006; Luczaj, 2006; Lonnee and Machel, 2006).

Due to differences in the tectonic backgrounds of various stratigraphic layers, several models of hydrothermal alteration have been established, including the “thrust fault compression model” (Ronchi et al., 2012; Lapponi et al., 2018), “extensional strike-slip fault control model” (Nurkhanuly and Dix, 2014), “volcanic activity-induced model” (Li et al., 2021), and “syndimentary extensional fault model” (Hips et al., 2016; Yang et al., 2020). Based on seismic interpretation results, the hydrothermal alteration of the Dengying Formation in the central Sichuan region is considered to follow the second model, with at least two phases of extensional strike-slip faulting, possibly accompanied by multiple episodes of hydrothermal alteration (Gu et al., 2023).

The Dengying Formation of the Ediacaran period in the Sichuan Basin contains the oldest known natural gas reserves globally and is a key contributor to China’s natural gas production (Ma et al., 2019; Wang et al., 2023). The discovery of the Anyue Gas Field marked the beginning of efficient exploration of China’s Ediacaran oil and gas systems, with recent exploration efforts gradually moving northward from the Anyue area (Ma et al., 2022; He et al., 2023; Zhang et al., 2024). In recent years, many scholars have recognized the presence of a highly abundant cratonic strike-slip fault system within the Ediacaran hydrocarbon system of the Sichuan Basin (Ma et al., 2018; Guan et al., 2022; Tian et al., 2024). This concept was first introduced by British scholars, who classified it as a distinct type of strike-slip fault based on plate tectonic environments (Cunningham and Mann, 2007). Cratonic strike-slip faults are usually found away from plate boundaries. They are generally considered to be pre-existing crustal faults that experience short-distance horizontal displacement due to localized stress within the plate, hence also called small strike-slip displacement faults (Deng et al., 2019; Wu et al., 2020). Because of their small scale, the seismic response characteristics of these faults are not as prominent as those of dip-slip faults (reverse and normal faults) or large strike-slip faults. Consequently, before the use of extensive 3D seismic data, these faults were often overlooked in hydrocarbon exploration. In recent years, strike-slip fault-controlled oil and gas fields in the Tarim Basin have achieved proven reserves of one billion tons (Wu et al., 2020; Jiang et al.,

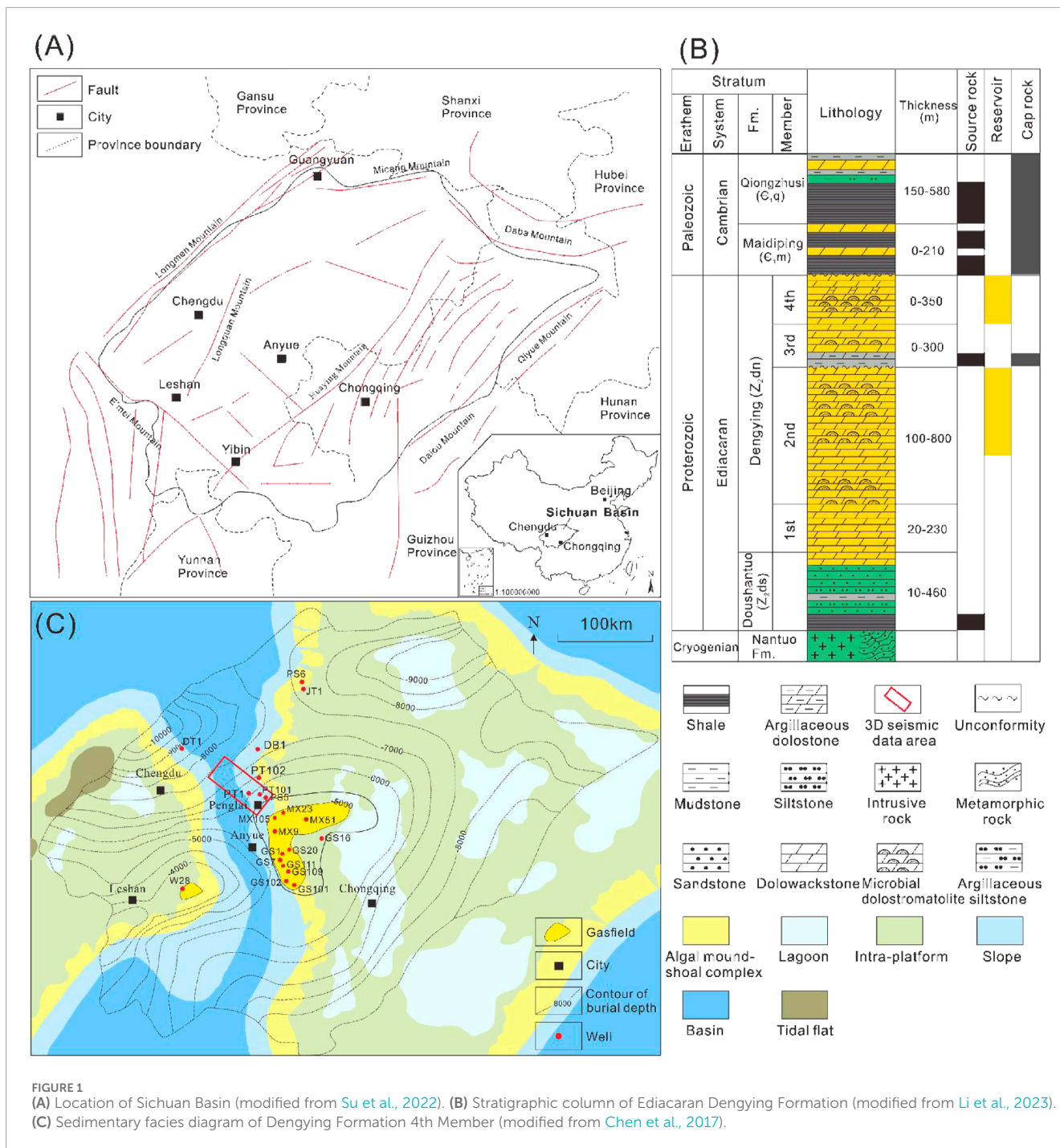
2020). This has increased interest in the study of strike-slip fault systems and their hydrocarbon control features in paleo cratonic basins.

Previous studies have indicated that the strike-slip fault system in Central Sichuan Basin has a complex origin and has undergone multiple faulting events (Jiao et al., 2021; Jiang et al., 2016; Ma et al., 2023). However, there has been limited research using chronological evidence to determine the fault formation periods. In recent years, the increasingly mature application of *in-situ* U-Pb dating technology to carbonates has enriched the chronological data for the Ediacaran hydrocarbon system (Deng et al., 2023; Shen et al., 2021; Gu et al., 2023), providing objective conditions for the integrated analysis of dating evidence and strike-slip faults. Strike-slip faults are believed to enhance the porosity and permeability of deep carbonate reservoirs (Ma et al., 2018), and facilitate communication between source rocks and reservoirs (Jiao et al., 2021). The discovery of strike-slip faults offers new insights for evaluating the Ediacaran hydrocarbon system, though it remains unclear how these faults influence reservoir formation. The impact of strike-slip faults on hydrocarbon accumulation conditions also requires further analysis. Additionally, the low resolution of seismic data in the Sichuan Basin makes it challenging to delineate the distribution of strike-slip faults, limiting their detailed analysis and evaluation.

This paper utilizes 3D seismic data from central Sichuan Basin to conduct seismic-geological response analysis and continuous seismic interpretation, identifying and mapping the distribution of strike-slip faults. Based on the interpretation results, the levels of strike-slip faults are classified, and their patterns are identified. The evolution of the strike-slip faults is elucidated. Additionally, the influence of these faults on the hydrocarbon system is revealed, including their control effects on various accumulation conditions. This study aims to provide a foundation for deploying exploratory strategies for fault-controlled hydrocarbon reservoirs.

Geological background

The study area is located in the Central Sichuan Basin, specifically in the northern part of the Anyue area (Figure 1A). Based on microbial algae content and sedimentary structure types, the Ediacaran Dengying Formation in the study area can be divided into four lithological members (Figure 1B). The 2nd and 4th members are primarily composed of microbial dolostones, such as dolostromatolites and oncolites. The 1st Member is mainly composed of dolowackstones (Gu et al., 2023). The 3rd Member is predominantly black mudstone/shale. Multiple phases of the Tongwan uplift during the late Ediacaran caused erosion and extensive karstification at the top of the 2nd and 4th members,



leading to the formation of large-scale unconformities. Due to varying intensities of erosion, the 3rd and 4th members are absent in some areas, resulting in an unconformable contact between the 2nd Member and the overlying Cambrian source rocks. In this context, the top of the 2nd and 4th members developed widespread paleo karst features, which were subsequently transformed into the source-associated mound-shoal complex reservoirs (or grain shoals) (Figure 1C). The Ediacaran-lower Cambrian strata in the Sichuan Basin are arranged in a bottom-up sequence, comprising the Doushantuo, Dengying, Maidiping, Qiongzhusi, Canglangpu, and Longwangmiao formations (Figure 2).

All these source rocks from Cambrian system have equivalent vitrinite reflectance values greater than 2.0%, indicating that they have reached the overmature stage (Wei et al., 2017; Guo et al., 2024). Recent geochemical studies on the bitumen within the reservoirs suggest that the overlying Cambrian Maidiping Formation and Qiongzhusi Formation mudstone/shale are the primary source rocks for the hydrocarbons in the Dengying Formation (Fang et al., 2024). The significant variation in the scale of source rock development also indicates that the Qiongzhusi Formation mudstone/shale are the largest source of hydrocarbons.

Chronostratigraphy	Lithostratigraphy		Lithology	Thickness (m)	Depositional Environment	Tectonic Movement
	Formation	Sym.				
Quaternary		Q				Late Himalayan
Neogene		Ng				Early Himalayan Late Yanshanyan
Paleogene		Pg				
Cretaceous		K				
Jurassic	Upper	Penglaizhen Suining	J ₃ p J ₃ sn	>650	Alluvial-lucustrine facies sandstones mudstones and shale	
	Middle	Shaximiao	J ₂ s	~2000		
	Lower	Ziliujing	J ₁ z	~760		
Triassic	Upper	Xujiahe	T ₃ x	~200	Marine carbonates evaporites and black shale and alternating marine and terrestrial facies clastics and coal-bearing bulidup	Late Indosinian
	Middle	Leikoupo	T ₂ l	~550		Early Indosinian
	Lower	Jialingjiang	T ₁ j	~950		Hercynian
		Feixianguan	T ₁ f	~400		Dongwu
Permian	Upper	Changxing Wujiaping	P ₃ ch P ₃ w	~330	Marine carbonates evaporites and black shale and alternating marine and terrestrial facies clastics and coal-bearing bulidup	Yunnan Caledonian Guangxi
	Middle	Maokou	P ₂ m	~400		
		Qixia	P ₂ q			
	Lower	Liangshan	P ₁ l			
Carboniferous		Huanglong	C ₂ h	~40		
Devonian			D	~20		
Silurian	Middle	Hanjiadian	S ₂ h	~1230		
	Lower	Xiaoheba	S ₁ x			
		Longmaxi	S ₁ l			
Ordovician			O	~360		
Cambrian			Є	~1800		
Ediacaran		Dengying		300 ~2500		Tongwan
		Doushantuo			Chengjiang	
Cryogenian						

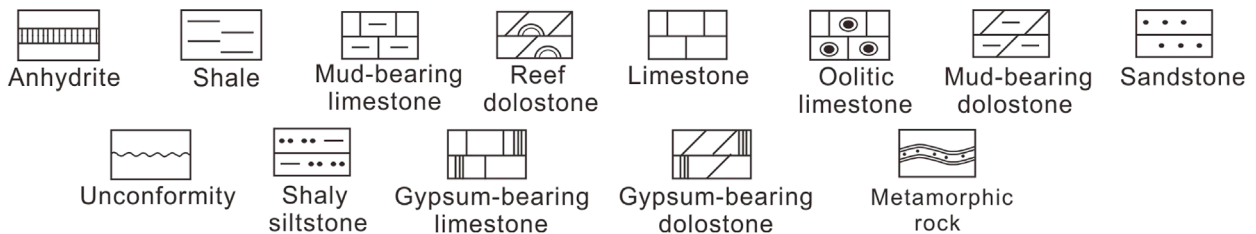


FIGURE 2 Stratigraphic column of the central sichuan basin (modified from Hao et al., 2008).

Samples and methods

Reservoir characterization

The studied wells carried out continuous coring in Ediacaran Dengying Formation. Core observation identified different lithology, including dolowackstone, microbial dolostromatolite, dololaminite, breccia dolostone, dolograinstone, and record the lithology combination of different members. 158 thin sections of core samples were made and the core observation results were further verified by Carl Zeiss Axio Observer D1 optical microscope (Oberkochen City, Germany). Observation and description of typical sections were made in the study area, with emphasis on sedimentary texture or structure.

High-resolution processing of seismic data

To identify faults within the Dengying Formation and its overlying and underlying strata, seismic data were first evaluated. The seismic data has a dominant frequency of 25 Hz, with an effective frequency range from 5 Hz to 58 Hz, and abundant low-frequency signals. The signal-to-noise ratio is generally high, and the data quality is good. However, the layer interfaces within the Dengying Formation are unclear, and the characteristics of faults, fault planes, and fault points are not well defined. As a result, a harmonic high-frequency recovery method was applied to process the seismic data from the 3D survey area (Figure 3). The method works by calculating the harmonics of the original signal (with frequencies as integer multiples of the base frequency) to enhance high-frequency information, and by calculating the subharmonics (with frequencies as fractional multiples) to enhance low-frequency information. The processed seismic data's effective frequency range was expanded from 6 Hz–58 Hz to 6 Hz–80 Hz, significantly improving resolution while preserving the original signal-to-noise ratio and low-frequency content. Moreover, this method preserves the relative amplitude relationships of the seismic data and restores the missing frequency components of the signal as accurately as possible (Figure 4). The use of high-resolution data across different frequency bands has made the identification of internal layer interfaces, mound-shoal features, and fault details much clearer.

Multi-scale fault identification based on frequency division technology

Seismic data at different frequencies can effectively characterize faults at various scales. As the frequency increases, more detailed information about faults and fractured zones becomes available. Therefore, in this study, frequency decomposition techniques were applied to identify faults at multiple scales. By integrating data from various frequency bands, fault information at different scales was extracted and combined to form a multi-scale fault detection model. The specific technical process is shown in Figure 5. To address the characteristics of small displacement and weak seismic response of strike-slip faults, seismic data was reprocessed to improve the resolution of strike-slip faults, followed by their identification

and detailed interpretation. Through analysis of seismic-geological responses of typical strike-slip faults, coherence and instantaneous amplitude were selected for seismic identification of strike-slip fault zones. Additionally, methods such as high-frequency, medium-frequency, and low-frequency seismic identification were used to detect small-scale strike-slip faults. Based on this, seismic interpretation of strike-slip faults in the Central Sichuan Basin was carried out.

Results

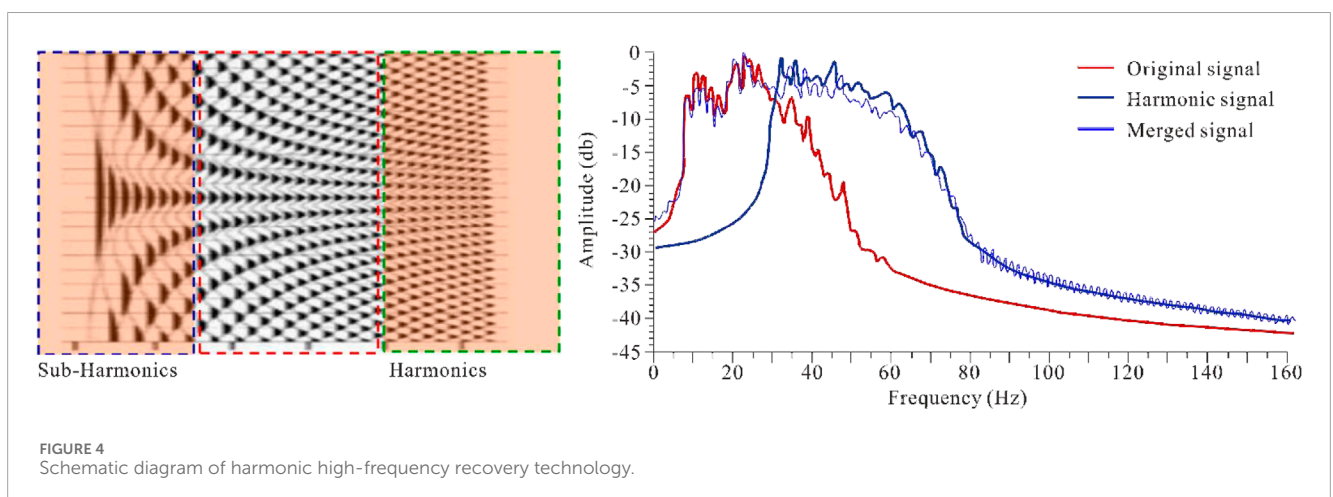
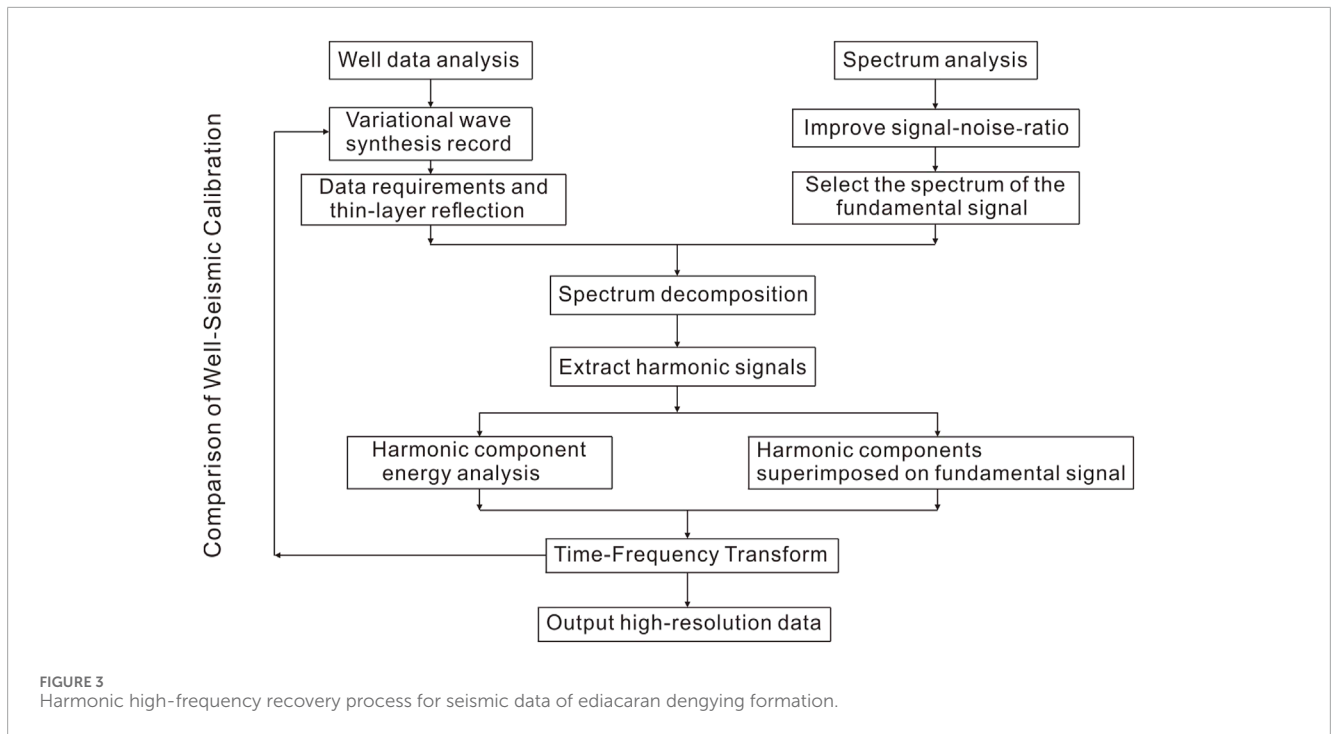
Algal mound-shoal reservoir characteristics

The lithological composition of the mound-shoal complex consists of alternating dolostromatolite and dolograinstone layers. The grain shoals are composed solely of dolograinstone. Core analysis, thin-section identification, and porosity measurements indicate that the Ediacaran Dengying Formation reservoir was formed through diagenetic alteration by meteoric freshwater, primarily in the context of mound-shoal complexes, grain shoals, and mounds (Figure 6). Dolowackstone represents an inter-complex (or shoal) environment with poor hydrodynamic conditions, resulting in extremely low primary porosity that hinders diagenetic alteration by fluids. The reservoir rock is primarily dolostromatolite, which is rich in dissolved vugs. Microscopic observations reveal the presence of numerous pores with diameters less than 2 mm (Figure 7A), in addition to the dissolved vugs (Figure 7B). Porosity is mainly distributed between 2% and 4%, accounting for 51.0% of the total sample set ($n = 147$). The reservoir's physical properties generally exhibit low porosity (<4%), with localized areas reaching higher porosity (>4%), but still higher than those found in the Anyue Gas Field. Permeability ranges from 0.009 to 0.857 mD, with an average of 0.172 mD and a median of 0.09 mD. The fractures are primarily structural (Figures 7C, D), and their association with dissolved pores and vugs creates favorable conditions for the formation of a reservoir (Figures 7E, F). Thus, the reservoir type in the Dengying Formation is classified as fracture-vug type (Figures 7G, H). The total thickness of the reservoir ranges from 155 m to 280 m.

Classification of strike-slip faults

This study employs frequency-domain multi-scale fault (and fracture) recognition techniques to enhance fracture interpretation accuracy and provide more detailed information on fault zones (Figure 8). The strike-slip fault at the platform-margin of the Dengying Formation extends roughly in an EW direction in plan view. These faults are characterized by early development and early disappearance in its geological history. The fault intersects different strata at various locations: it extends downward to the base of the Pre-Ediacaran system and upward, terminating at the Middle Permian Qixia Formation and Lower Triassic Feixianguan Formation.

Strike-slip faults are typically nearly vertical, but variations in their orientation along strike result in both normal and reverse faulting. When the strike-slip fault plane has the same dip direction,



it may appear as a normal fault in one cross-section and as a reverse fault in another. The relative displacement, slip type, and direction differ between adjacent cross-sections. The fault's dip direction fluctuates frequently between multiple orientations, such as southeast, vertical, southeast, and northwest, a phenomenon referred to as the “ribbon effect”. In the study area, identified strike-slip faults display various forms on seismic profiles, including high-steep-erect structures, negative flower structures, and inclination reversal structures.

The high-steep-erect structure is the most common characteristic of strike-slip faults in the study area. These faults are mostly transtensional type, with nearly vertical profiles and fault dips greater than 80°. The fault extends upward into the Cambrian or Permian strata and downward directly to the base of the Pre-Ediacaran system. Its morphology becomes progressively

steeper with depth (Figure 9). The negative flower structure is a composite profile formed by the main and branching strike-slip fault segments, and it is considered one of the key indicators for identifying strike-slip faults (Harding, 1990; Xiao et al., 2017). The widespread development of the negative flower structure indicates that strike-slip faults form in an extensional-shear tectonic setting. The inclination reversal structure is a common fault type in the study area, characterized by two normal faults with opposite dips, forming a small graben. The main displacement zone of the strike-slip fault belt extends linearly in plan view, with the associated strike-slip structural features confined to a limited area near the main displacement zone, giving the entire fault structure a banded appearance.

For example, in the Dengying 2nd Member, three groups of strike-slip faults with different orientations have been identified and

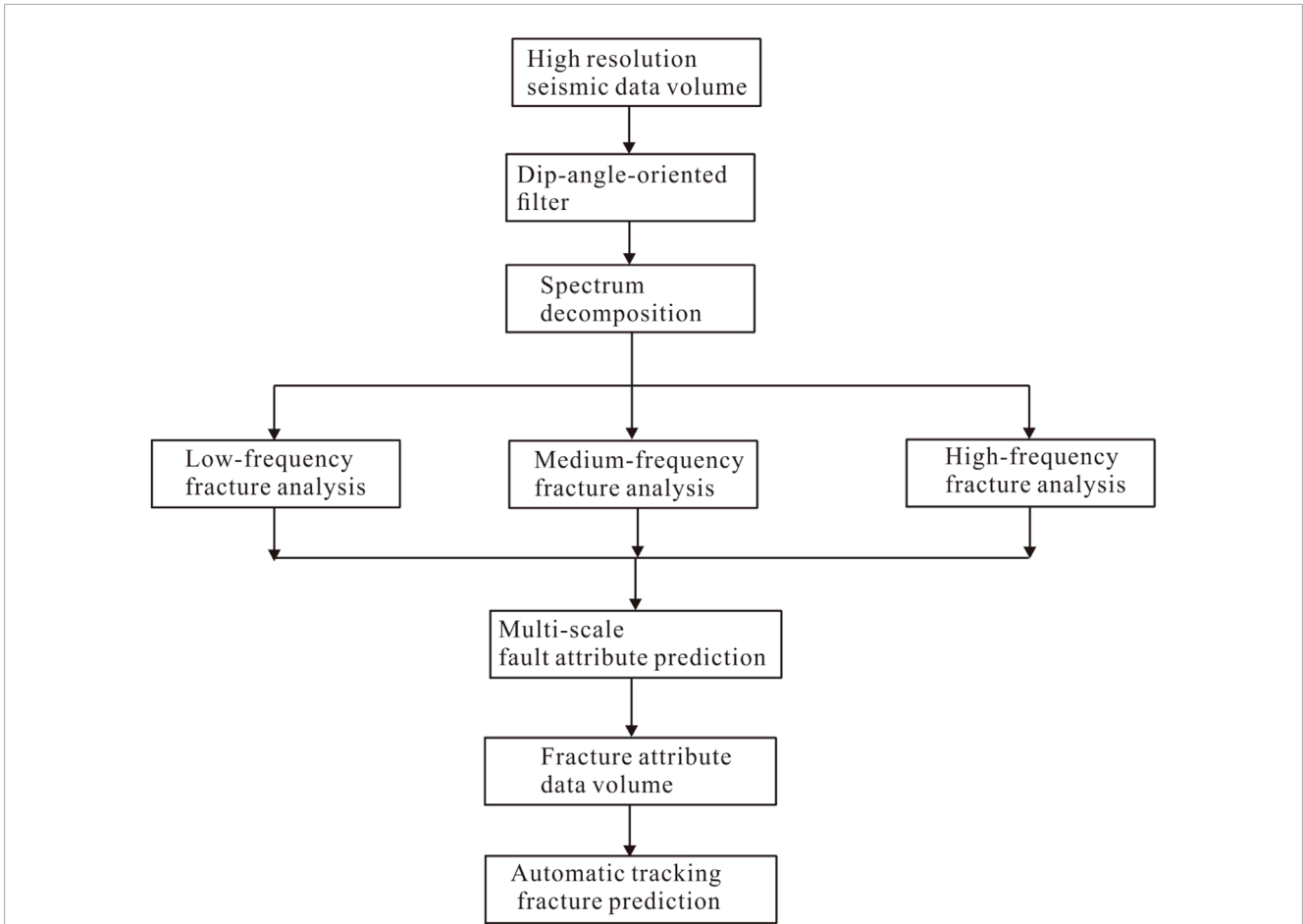


FIGURE 5
Technological process of frequency division and multi-scale fault (and fracture) identification.

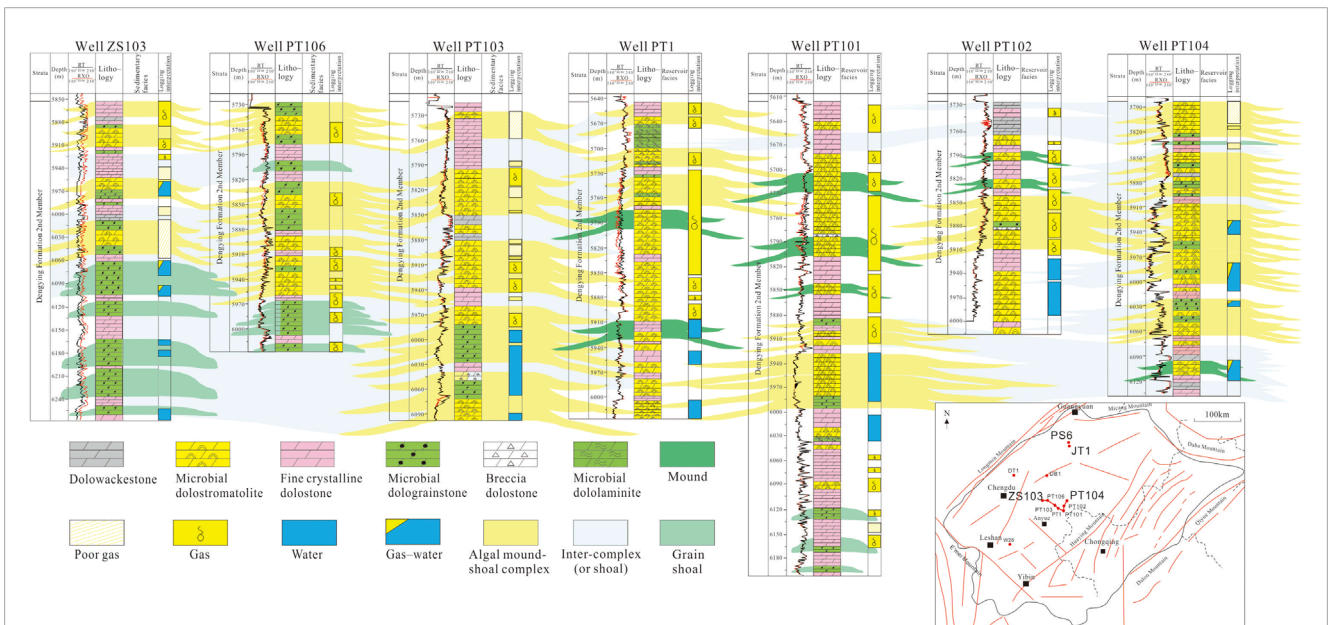


FIGURE 6
Distribution characteristics of mound-shoal complex, mound and grain shoal in ediacaran dengying formation.

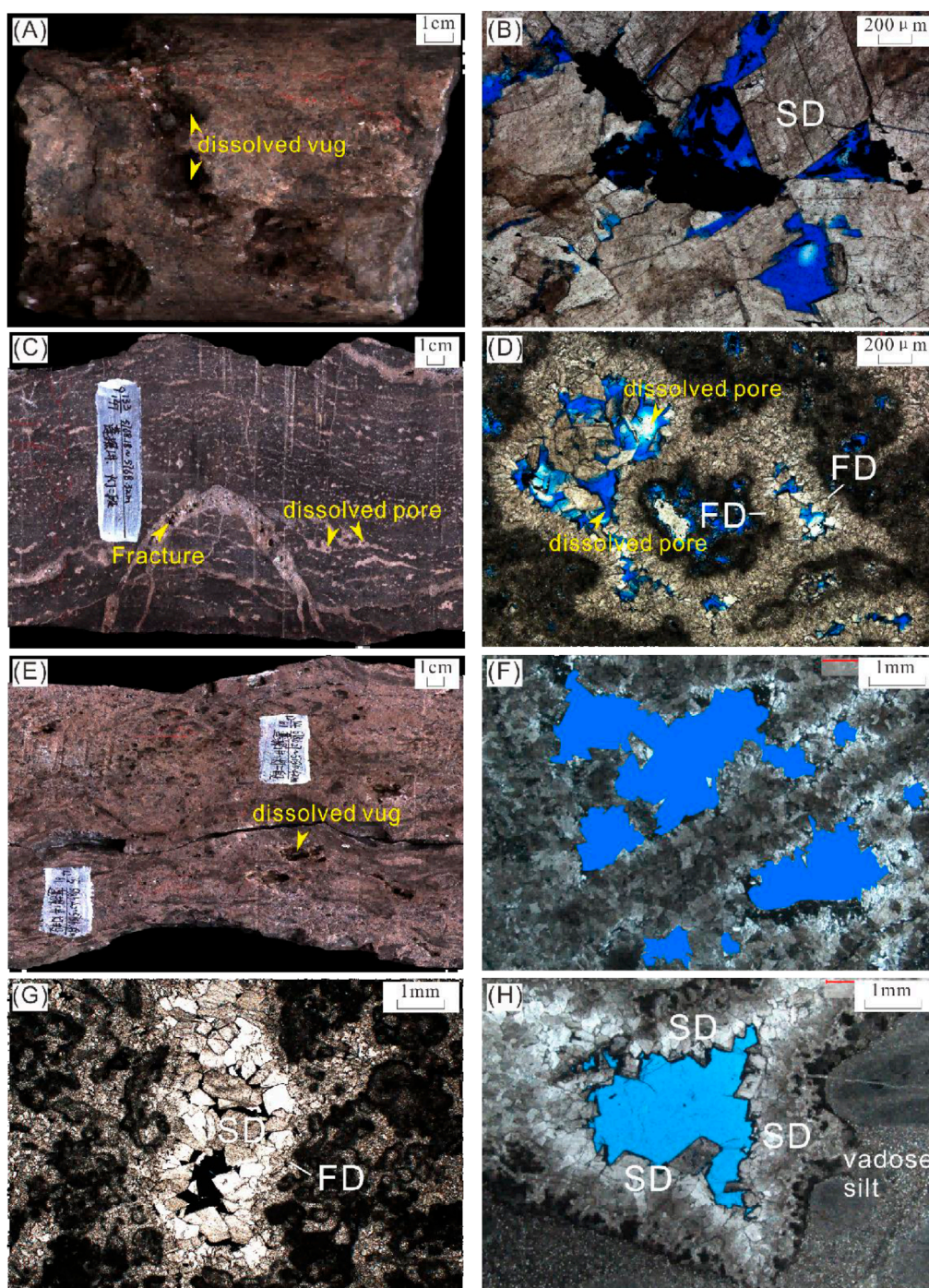
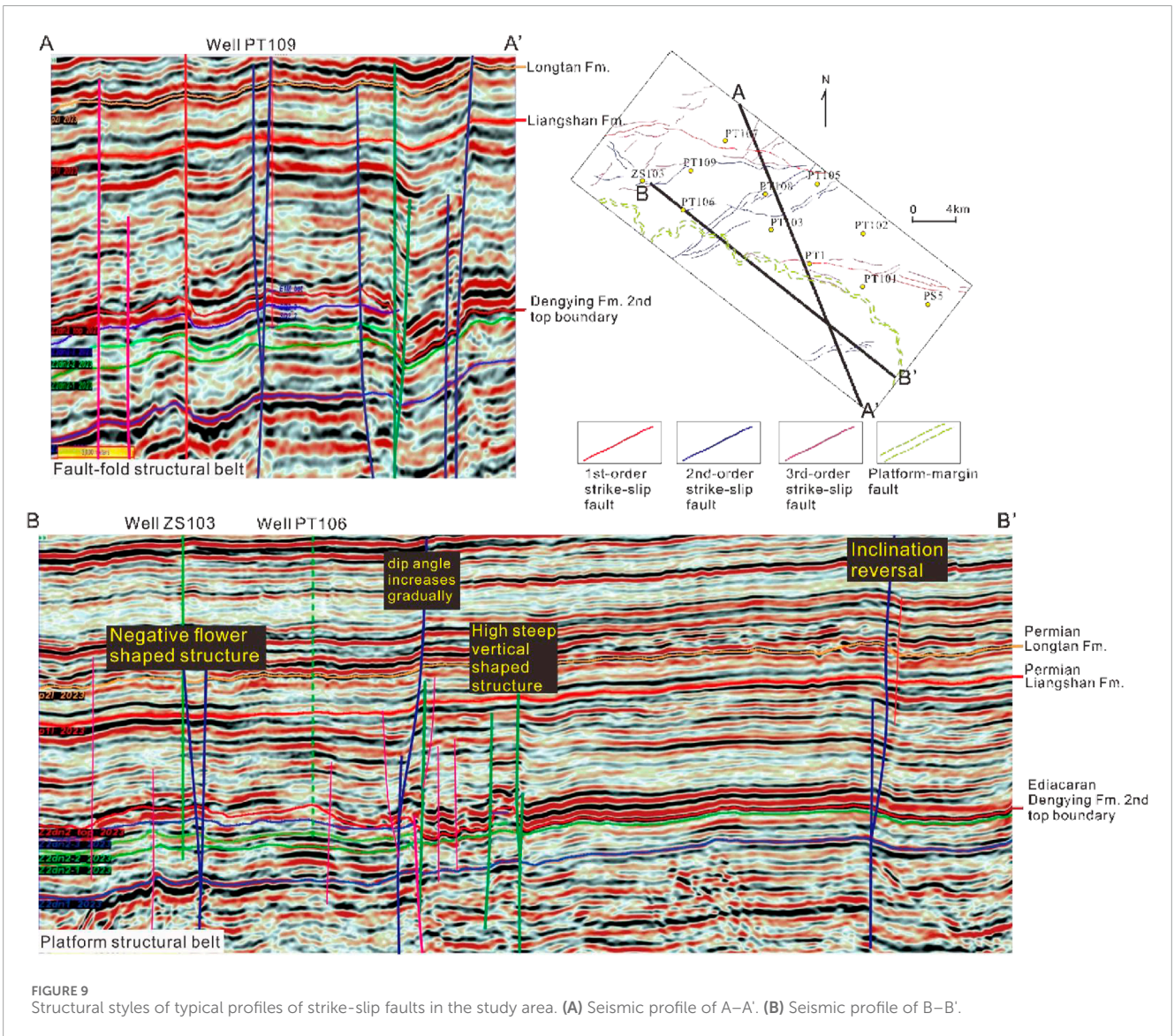
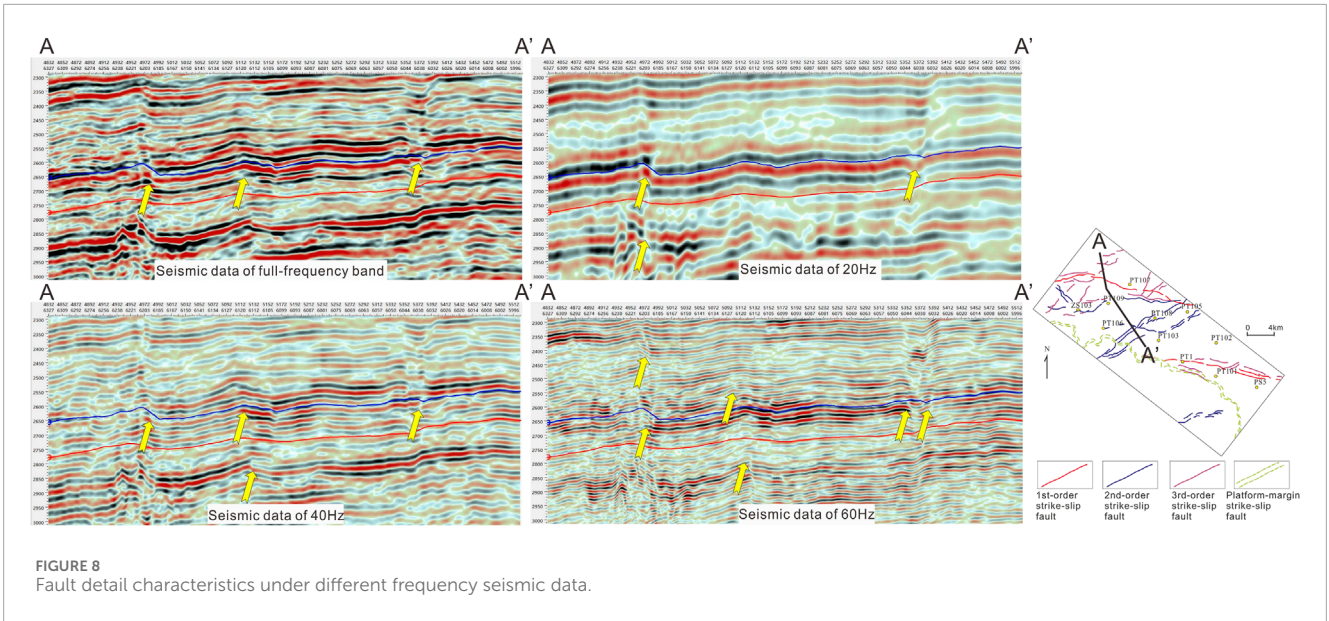


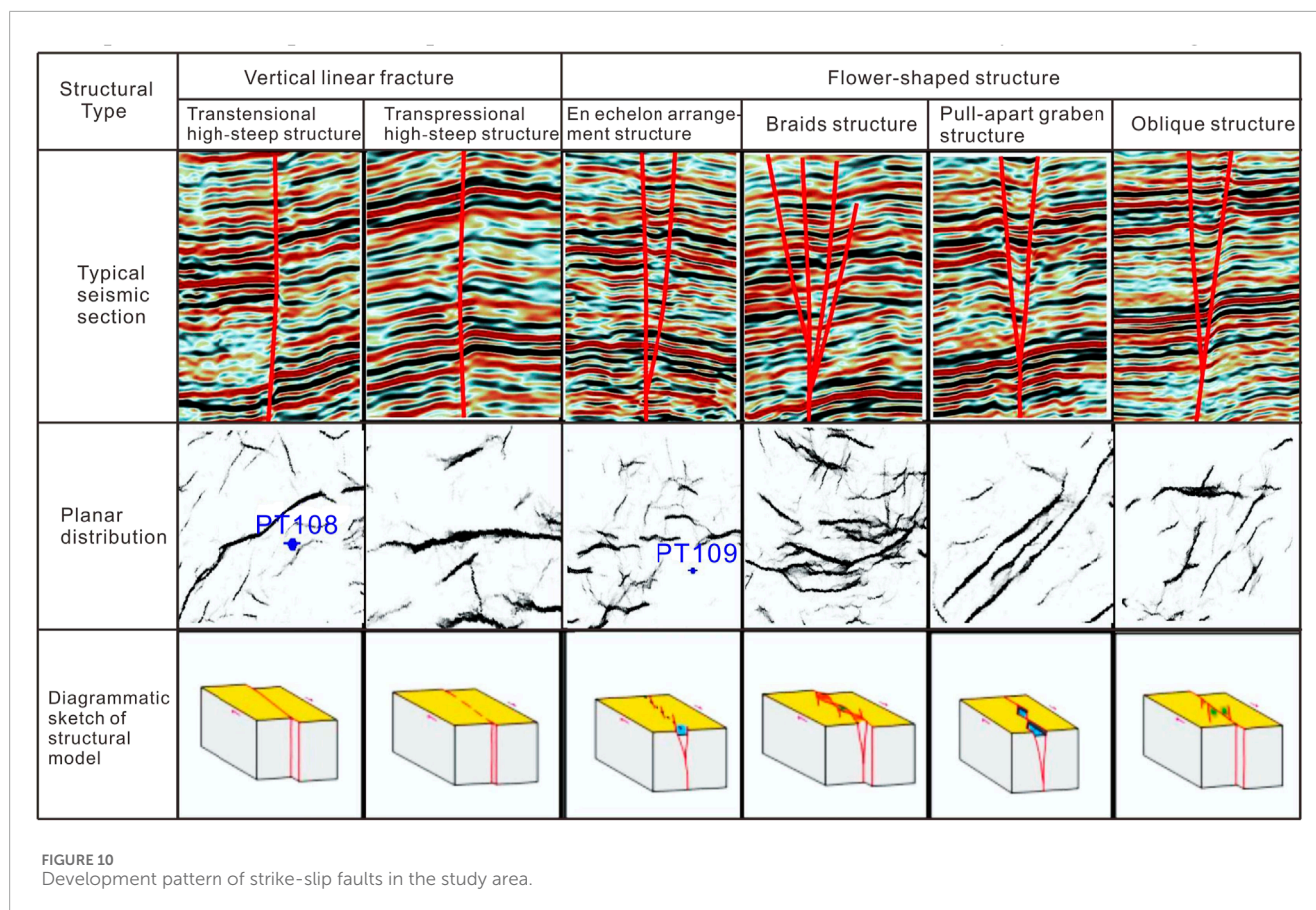
FIGURE 7

Petrological characteristics of mound-shoal complex reservoir in ediacaran dengying formation. (A) Vugs with a diameter of more than 1 cm and pores with a diameter of less than 2 mm can be observed on the drilling core, Well PT1, 2nd Member, 5,767.94 m. (B) The cementation of saddle dolomite leads to the reduction of karst vugs to karst pores, Well PT1, 2nd Member, 5,767.94 m. (C) Structural fractures and dissolved pores, Well PT1, 2nd Member, 5,768.32 m. (D) Dissolved pores, Well PT1, 2nd Member, 5,768.32 m. (E) Structural fractures and dissolved vugs, Well PT1, 2nd Member, 5,786.49 m. (F) Dissolved vugs, Well PT1, 2nd Member, 5,786.49 m. (G) Vugs filled by fibrous dolomite and saddle dolomite, Well ZS101, 2nd Member, 6,244.93 m. (H) Vugs filled by vadose silt and saddle dolomite, Well PT101, 2nd Member, 5,725.21 m.

classified. The primary strike-slip fault follows a NWW-SEE trend in plan view. In the eastern part of the study area, the primary fault extends from the base to the Permian layers, while in the central-western part, it extends from the base to the Triassic system (Figure 9). On seismic profiles, the primary fault appears vertical

and exhibits a linear characteristic in plan view. The first group of 2nd-order faults trends roughly east-west in plan view and connects with the 1st-order fault to the east. The displacement of the 2nd-order faults decreases with depth, and by the Permian, only axial twists of the same-phase structure are observed. Along the strike





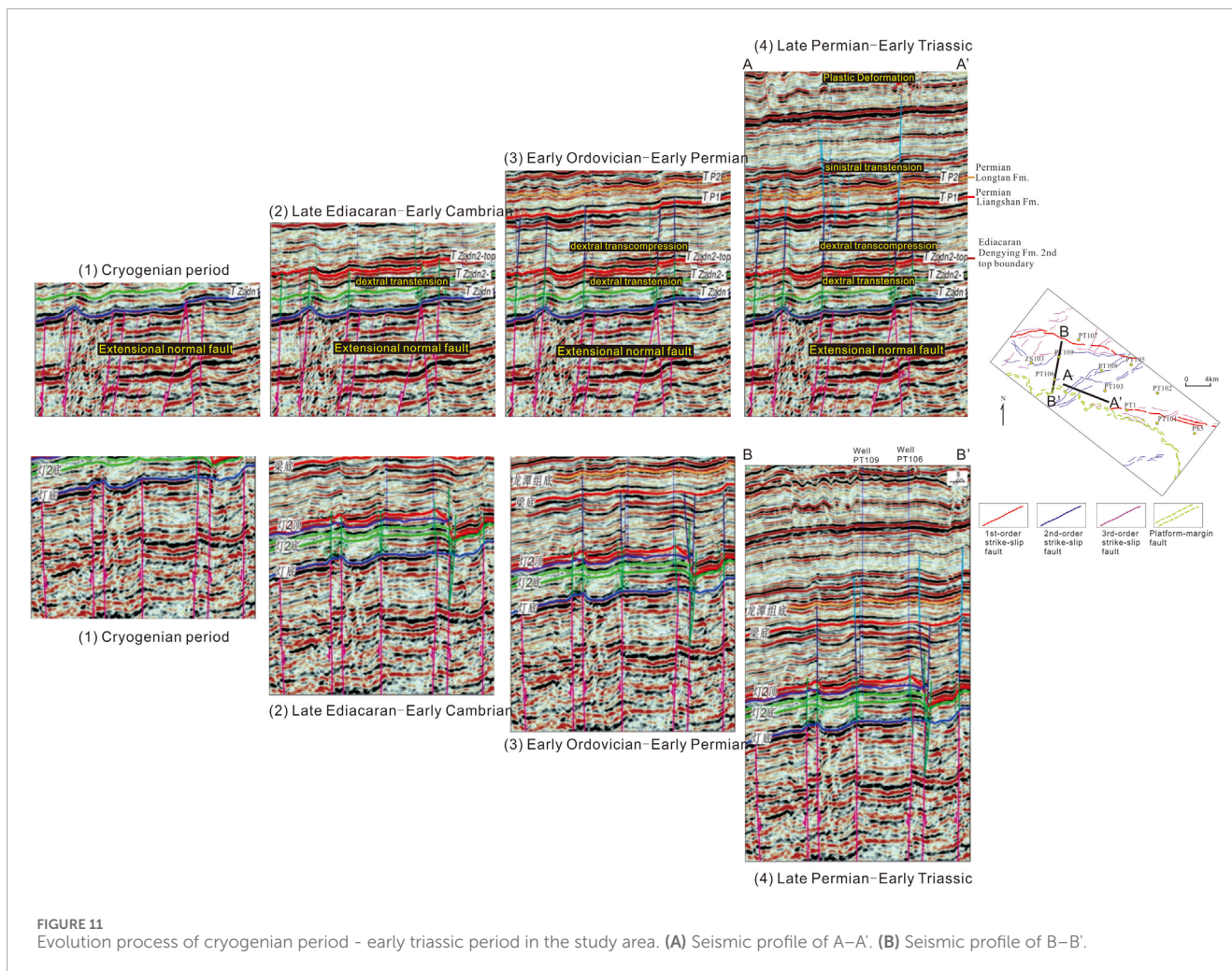
direction, the “ribbon effect” is visible on seismic profiles. On seismic profiles, the 2nd-order faults exhibit vertical characteristics, with a linear appearance in plan view. The second group of 2nd-order faults trends northeast-southwest in plan view and intersects the 1st-order fault to the east (Figure 9). On seismic profiles, this group of 2nd-order faults shows larger displacement in the western section, decreasing toward the east. On seismic profiles, the secondary faults take on a vertical-oblique-Y-shaped form. In plan view, this group of 2nd-order faults also exhibits a linear characteristic.

Strike-slip fault pattern and evolution process

The South China Block, part of the Sichuan Basin, was involved in the assembly and rifting of the Rodinia supercontinent. The South China Block is considered to be part of an active continental margin, with a temporal and spatial connection to the subduction system of Rodinia (Cawood et al., 2013; Cawood et al., 2016; Li et al., 2018; Konopásek et al., 2018; Liu et al., 2019). The subduction forces from the edge of the South China Block are transmitted inward, and differential compressive deformation may directly lead to the formation of northwest-trending strike-slip faults (Ma et al., 2023). The planar patterns of strike-slip faults can be categorized into linear, en echelon, and oblique structures (Yang et al., 2022). On seismic

profiles, strike-slip faults are typically observed as vertical (or steep) linear faults or flower-shaped structures (Figure 10). The strike-slip faults in the Dengying Formation also exhibit characteristics of normal faults. Vertical (or steep) linear faults can further be classified into transensional high-steep structures and transpressional high-steep structures. The transensional high-steep structure has a single fault plane with a dip close to 90°. When displacement is significant, it can form small, single-fault basins, but its linear extent in plan view is limited. The transpressional high-steep structure also has a single fault plane with a dip near 90°, but with smaller displacement. This structure forms small fault noses and folds, but its linear extent in plan view is limited. Flower-shaped structures can be further divided into en echelon, braid, pull-apart graben, and oblique structures (Figure 10). In the en echelon structure, secondary faults intersect the central line of the fault zone at a small angle, with the strike-slip fault converging downward. In the braid structure, strike-slip faults intersect each other, forming a narrow, elongated fault zone. In the pull-apart graben structure, the extensional-shear faults converge downward, but the scale is small. In the oblique structure, the adjustment faults formed by the main fault appear Y-shaped on seismic profiles. In plan view, the main fault intersects the secondary faults at an angle.

The evolution of strike-slip faulting in the Central Sichuan Basin consists of four distinct stages. There are variations in fault activity across the different evolutionary stages. This is evident in the episodic and intermittent activation of strike-slip

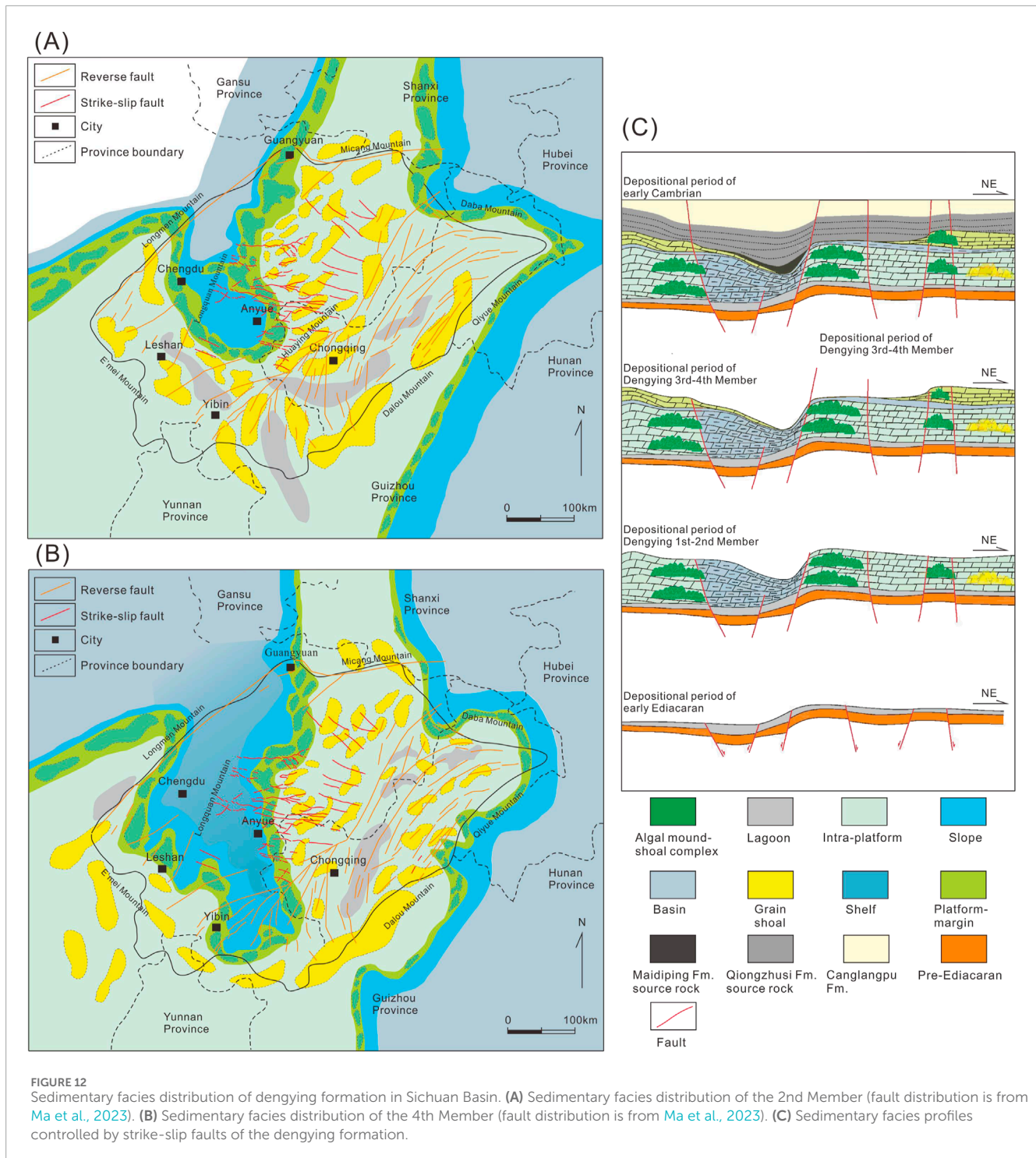


faults during different stages. During the Cryogenian period, tectonic activity was characterized by rifting. The northwest-southeast trending foreland-retreat subduction of the original Tethys Ocean formed the NE and NNE rift systems (normal faults), which, together with NW strike-slip faults, provided the foundation for later strike-slip fault development. During the late Ediacaran to early Cambrian (Figure 11), tectonic activity was dominated by dextral transtensional strike-slip motion. The Yangtze Plate rotated clockwise, activating NE- and NW-trending faults under east-west extensional stress, resulting in dextral strike-slip motion. During the early Ordovician to early Permian, tectonic motion was characterized by dextral, weak transpressional strike-slip movement. North-south compression formed east-west trending extensional faults, which continued to activate NE- and NW-trending faults, resulting in dextral transpressional strike-slip activity (Figure 11). During the late Permian to early Triassic, tectonic movement was characterized by sinistral transtensional strike-slip activity. Influenced by the Emei Rift (mantle plume and the formation of the Emei large volcanic rocks), the Central Sichuan Basin experienced NW-SE extension, forming NW-trending transtensional structures.

Discussion

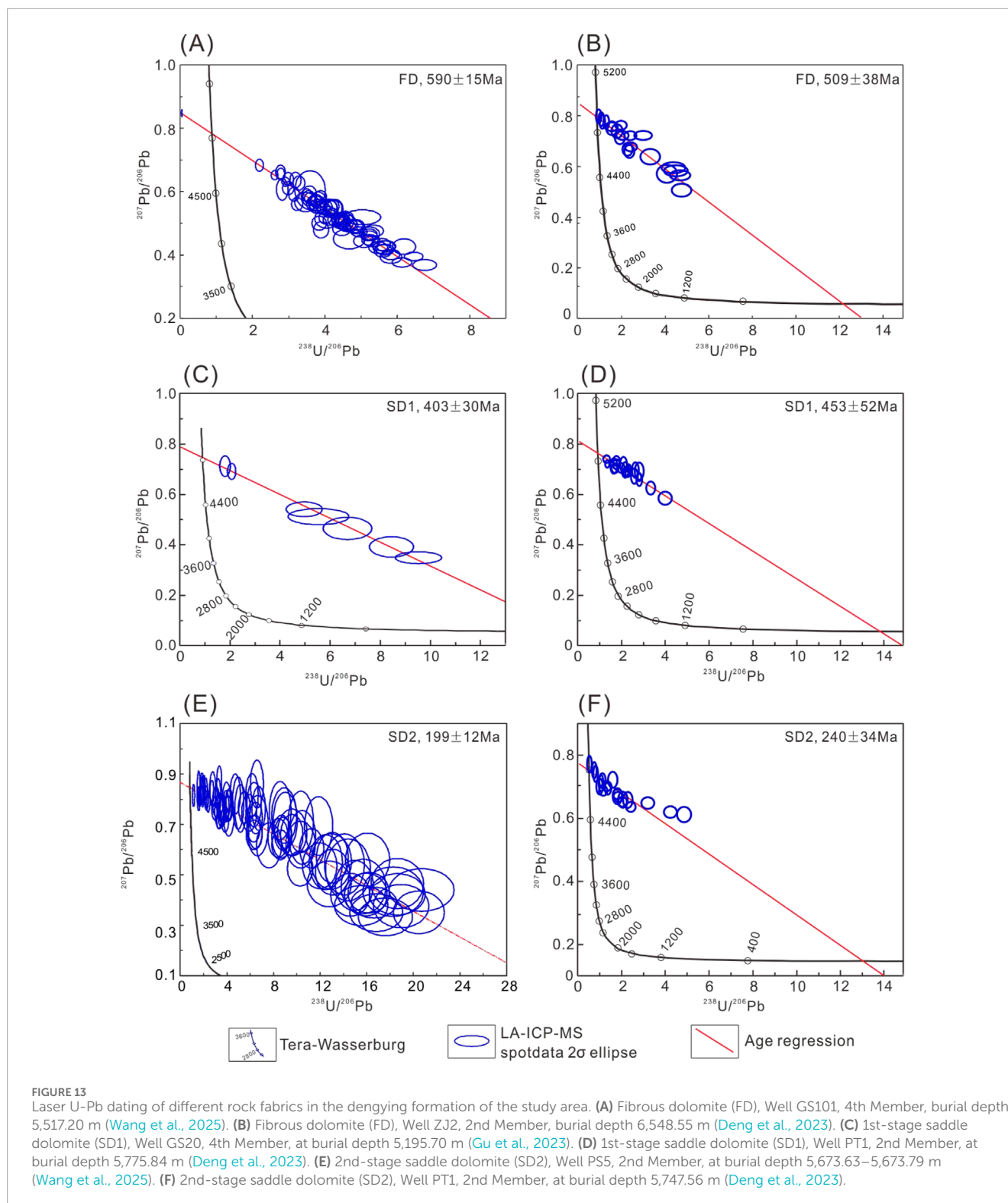
Controlling effect on deposition of mound-shoal complex

The aulacogen, formed during the Cryogenian period, developed above the Pre-Ediacaran rift basin and began taking shape during the deposition of the Duanshantou Formation, subsequently influencing the sedimentary patterns of the overlying Ediacaran Dengying Formation (Figure 12A). The platform-margin fault controls the north-south distribution of the platform-margin facies. Within the aulacogen, undercompensated deposits occur, with platform-margin sediments on either side. Additionally, the mound-shoal complex is segmented by east-west trending strike-slip faults and is distributed in an east-west belt pattern (Xie et al., 2022). The hydrodynamics along the platform-margin are strong. During frequent sea-level fluctuations, the mound-shoal complex at the platform-margin is prone to subaerial exposure, subjecting it to atmospheric freshwater dissolution. The closer the feature is to the platform-margin fault, the more frequent its exposure, leading to stronger dissolution and fracturing. Therefore, the platform-margin



faults macroscopically control the distribution of high-quality reservoirs. The mound-shoal complex primarily develops algae mounds associated with biological construction and dolograins related to grain shoals. The abundant algae and their binding actions create significant framework pores, providing the foundation and storage space for high-quality reservoirs. Strike-slip faults along the platform margin and within the platform itself have formed a paleogeomorphology with varying elevations (Figure 12B). The high points of this paleogeomorphology experience strong

hydrodynamics, creating the material foundation for reservoir formation, such as mound-shoal complexes and grain shoals. The transitional zones between the high and low points of the paleogeomorphology facilitate the movement of atmospheric freshwater during the surface processes, promoting the large-scale development of karst reservoirs (Figure 12B). Simultaneously, the numerous fractures formed by strike-slip faults help expand pores into dissolved vugs, enhancing both permeability and porosity within the reservoir.



Controlling effect on deposition of source rock

The aulacogen formed by the platform-margin fault entered its infill and overall subsidence phases during the early Cambrian. The aulacogen features a deep-water environment, characteristic

of a deep shelf setting. In this environment, the Maidigping and Qiongzhusi Formations were deposited (Figure 12C). As a result, the aulacogen controlled the spatial distribution of high-quality source rocks in the Maidigping and Qiongzhusi Formations of the Cambrian. The organic-rich source rock within the aulacogen is thick, while the thickness gradually decreases toward the sides. The

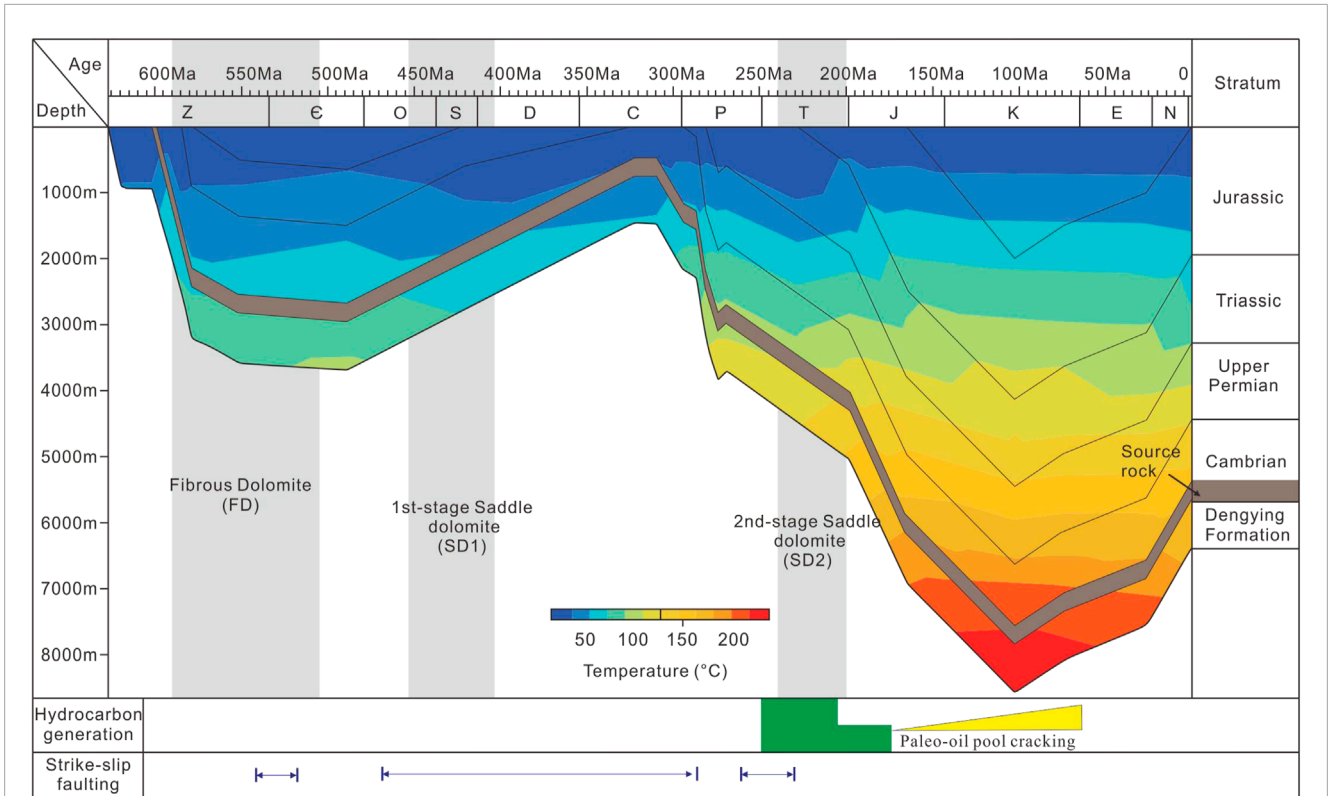


FIGURE 14 Depositional, burial and diagenetic history the Dengying formation of the study area (modified from Fan et al., 2022; Guo et al., 2025).

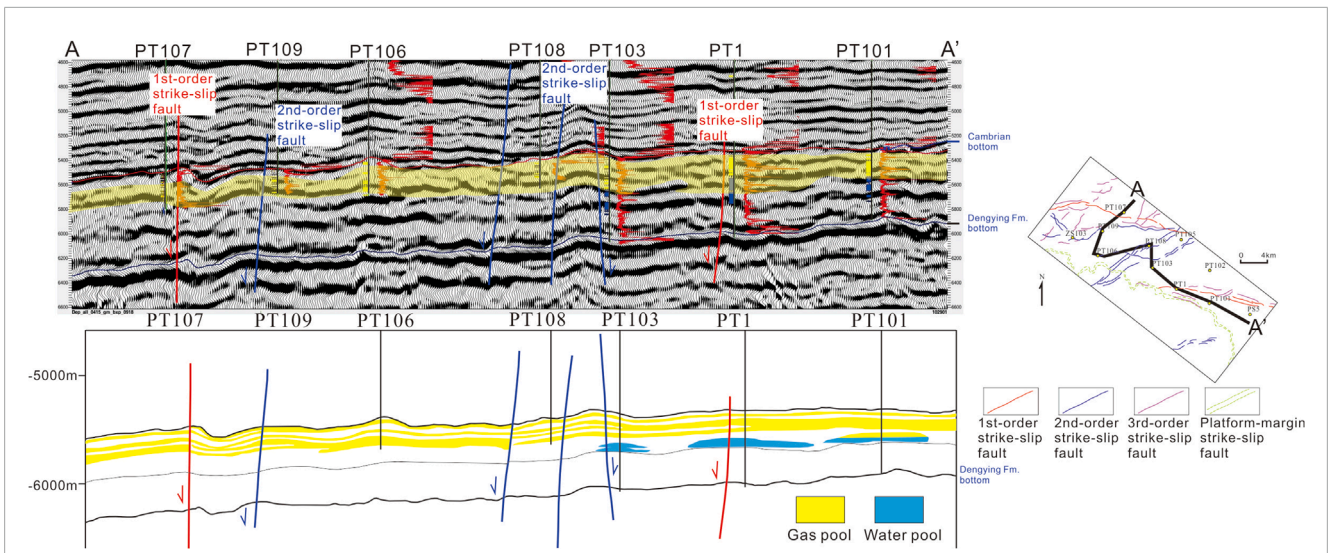


FIGURE 15 Cross-well profile of Dengying formation gas pool.

thickness of the source rocks in the Maidigping and Qiongzhusi Formations within the aulacogen ranges from 150 to 700 m, increasing progressively to the north. For example, the Maidigping and Qiongzhusi source rock thicknesses are 545 m in the Well GS17, 380 m in the Well CS1, and 473 m in the Well PT1, all within the aulacogen. In contrast, at the margin of the aulacogen, the source

rock thicknesses in the Qiongzhusi Formation are 267 m in the Well JT1, 238 m in the Well MS1, and 130 m in the Well GS1 (Xie et al., 2022). The total organic carbon (TOC) content in the Maidigping Formation ranges from 0.70% to 4.00%, with an average of 1.67%. The TOC content in the Qiongzhusi Formation ranges from 0.50% to 8.49%, with an average of 1.95%.

Controlling effect on diagenetic alteration

To investigate the impact of strike-slip faults on geological bodies such as mound-shoal complexes, U-Pb absolute ages of multiple cementation phases were collected. The fibrous dolomite cement (FD) along the edges of dissolved pores and vugs formed during the surface diagenesis phase was shown to have precipitated directly from seawater (Ding et al., 2019). The absolute ages of fibrous dolomite (FD) range from 590 ± 15 Ma to 509 ± 38 Ma (Figure 7D), indicating that the Tongwan uplift occurred before 590 Ma (Figures 13A, B). Some reports suggest that the surface diagenesis phase lasted more than 5 million years (He et al., 2023). The dextral transtensional strike-slip activity during the late Ediacaran to early Cambrian coincided with the timing of the Tongwan uplift. Under the guiding effect of strike-slip faults, large-scale atmospheric freshwater flow and water-rock interactions along the fault zones facilitated the development of karst fractures and vugs (Gu et al., 2019), leading to the formation of high-porosity, high-permeability fracture-vug reservoirs. The dextral transpressional strike-slip faults during the early Ordovician to early Permian represent inherited tectonic activity. However, due to the weak and small-scale fault activity, these faults mainly developed along the main strike-slip fault, exerting a limited but notable reworking effect on the reservoir. U-Pb dating identified several ages of saddle dolomite from the early Ordovician to Silurian (Figures 13E, F), suggesting the presence of a significant hydrothermal event that may have had a constructive impact on the reservoir (Figures 13C, D). The sinistral transtensional strike-slip faults and associated 2nd-stage hydrothermal activity during the late Permian to early Triassic had minimal impact on the reservoir (Figure 14), as evidenced by mineral fillings represented by 2nd-stage saddle dolomite (SD2) (Figure 7B). However, this stage of strike-slip faulting overlaps with the hydrocarbon generation period, contributing significantly to hydrocarbon accumulation (Figure 14). Systematic analysis of the petrographic features of cores and thin sections reveals that the hydrothermal alteration of the matrix dolomite of the Dengying Formation varies under the control of strike-slip faults. Under the control of strike-slip faults, the hydrothermal alteration of microbial dolostromatolites is primarily characterized by hydrothermal recrystallization, fragmentation and granulation, and cementation of fractures and vugs. Hydrothermal alteration of dolowackstone is dominated by processes such as hydraulic fracturing, layer-parallel replacement, dissolution, and the filling of associated minerals, leading to a dissolution-fill composite modification. The primary types of reservoir space created by hydrothermal alteration are dissolution pores, caves, and structural fractures. Effective connectivity between dissolution pores, caves, and network fractures (originating from strike-slip faulting) can form high-quality dolomite reservoirs.

Controlling effect on hydrocarbon accumulation

On one hand, multiple high-quality source rock units from the Paleozoic in the Sichuan Basin are in direct contact or have overlapping distributions with Ediacaran reservoirs vertically. Strike-slip faults connect deep hydrocarbon sources with underlying

carbonate reservoirs, forming a vertical migration and accumulation system. On the other hand, the aulacogen formed by the strike-slip faults allows lateral contact between source rocks and reservoirs (Figure 12), further enhancing hydrocarbon migration efficiency and facilitating large-scale accumulation. Previous studies suggest that the Dengying 3rd Member is composed of siltstone. The presence of strike-slip faults allows the Dengying 3rd Member to serve as a carrier bed for hydrocarbons, enhancing the upward migration and accumulation efficiency. Additionally, some inherited strike-slip faults extend upward into the Permian, connecting the Ediacaran, Lower Cambrian, Ordovician-Silurian source rocks with Permian traps, forming a multi-layered vertical composite accumulation system (Jiao et al., 2021).

Laterally, the NWW-striking strike-slip faults connect the hydrocarbon source center of the aulacogen with mound-shoal complex reservoirs within the platform, aiding hydrocarbon migration within the platform. Due to their early formation and stabilization, along with minimal Cenozoic disruption, strike-slip faults are conducive to the preservation of natural gas. The sinistral transtensional strike-slip faults during the late Permian to early Triassic overlap with the hydrocarbon generation period, significantly influencing the formation of paleo-oil pools. These strike-slip faults caused differences in the gas-water interfaces on either side of different mound-shoal complexes or even within the same complex. For example, in the PT1 well area on the eastern side of the fault (Figure 15), only one gas-water system exists, while multiple gas-water systems are found on the western side of the fault.

Conclusions

- (1) The strike-slip faults display various forms on seismic profiles, including high-steep-erect structures, negative flower structures, and inclination reversal structures. The planar patterns of strike-slip faults can be categorized into linear, en echelon, and oblique structures. Vertical (or steep) linear faults can further be classified into transtensional high-steep structures and transpressional high-steep structures. Flower-shaped structures can be further divided into en echelon, braid, pull-apart graben, and oblique structures. The evolution of strike-slip faulting in the Central Sichuan Basin can be divided into four distinct stages: (1) a rifting stage during the Cryogenian, (2) a dextral transtensional strike-slip stage from the late Ediacaran to early Cambrian, (3) a dextral, weak transpressional strike-slip stage from the early Ordovician to early Permian, and (4) a sinistral transtensional strike-slip stage during the late Permian to early Triassic.
- (2) The aulacogen, formed during the Cryogenian, controlled the distribution of the mound-shoal complex of the Dengying Formation and the thickness zones of the Cambrian hydrocarbon source rocks. The strike-slip faults in the first stage facilitated direct lateral and vertical contact between the overlying hydrocarbon source rocks and reservoirs, significantly enhancing the migration and accumulation efficiency of hydrocarbons. The strike-slip faults in the second stage controlled the distribution of ancient sedimentary paleogeomorphology and favorable karst locations. The strike-slip faults in the third stage governed the distribution of gas

and water. The sinistral transtensional strike-slip faults during the late Permian to early Triassic overlap with the hydrocarbon generation period, significantly influencing the formation of paleo-oil pools. These strike-slip faults caused differences in the gas-water interfaces on either side of different mound-shoal complexes or even within the same complex.

Data availability statement

The original contributions presented in the study are included in the article/supplementary material, further inquiries can be directed to the corresponding author.

Author contributions

YC: Conceptualization, Investigation, Writing – original draft. JL: Conceptualization, Methodology, Project administration, Writing – original draft. FL: Formal Analysis, Methodology, Writing – review and editing. LW: Investigation, Validation, Writing – review and editing. XZ: Investigation, Validation, Visualization, Writing – review and editing.

Funding

The author(s) declare that financial support was received for the research and/or publication of this article. This study was funded

References

- Cawood, P. A., Strachan, R. A., Pisarevsky, S. A., Gladkochub, D. P., and Murphy, J. B. (2016). Linking collisional and accretionary orogens during Rodinia assembly and breakup: Implications for models of supercontinent cycles. *Earth Planet. Sci. Lett.* 449, 118–126. doi:10.1016/j.epsl.2016.05.049
- Cawood, P. A., Wang, Y. J., Xu, Y. J., and Zhao, G. (2013). Locating South China in Rodinia and Gondwana: A fragment of greater India lithosphere? *Geology* 41 (8), 903–906. doi:10.1130/G34395.1
- Chen, Y., Shen, A., Pan, L., Zhang, J., and Wang, X. (2017). Features, origin and distribution of microbial dolomite reservoirs: a case study of 4th Member of Sinian Dengying Formation in Sichuan Basin, SW China. *Mar. Petroleum Geol.* 44 (5), 745–757. doi:10.1016/s1876-3804(17)30085-x
- Cunningham, W. D., and Mann, P. (2007). *Tectonics of strike-slip restraining and releasing bends*. London: The Geo-logical Society of London, 13–142.
- Davies, G. R., and Smith Jr, L. B. (2006). Structurally controlled hydrothermal dolomite reservoir facies: an overview. *AAPG Bull.* 90 (11), 1641–1690. doi:10.1306/05220605164
- Deng, B., Wu, J., Li, W., Wu, P., Tian, T., Jiang, H., et al. (2023). U-Pb dating and trapped hydrocarbon inclusions in carbonate for petroleum accumulation: case study from the Sinian Dengying Formation in the central Sichuan Basin. *Nat. Gas. Geosci.* 34 (11), 1887–1898. doi:10.11764/j.issn.1672-1926.2023.07.007
- Deng, S., Li, H., Zhang, Z., Zhang, J., and Yang, X. (2019). Structural characterization of intracratonic strike-slip faults in the central Tarim Basin. *AAPG Bull.* 103 (1), 109–137. doi:10.1306/06071817354
- Ding, Y., Chen, D., Zhou, X., Guo, C., Huang, T., and Zhang, G. (2019). Cavity-filling dolomite speleothems and submarine cements in the Ediacaran Dengying microbialites, South China: responses to high-frequency sea-level fluctuations in an aragonite–dolomite sea. *Sedimentology* 66, 2511–2537. doi:10.1111/sed.12605
- Fan, J., Jiang, H., Lu, X., Liu, Q., Liu, S., Ma, X., et al. (2022). Pressure evolution and hydrocarbon accumulation process of Sinian Dengying Formation gas reservoirs in the Penglai area, Sichuan Basin. *Nat. Gas. Ind.* 42 (12), 32–43. doi:10.3787/j.issn.1000-0976.2022.12.004
- Fang, X., Deng, B., Geng, A., Liu, S., Wang, P., Liang, X., et al. (2024). Geochemical properties, mechanism of formation, and source of solid bitumen in the Ediacaran Dengying Formation from the central to northern Sichuan Basin, China. *Mar. Petroleum Geol.* 159, 106573. doi:10.1016/j.marpetgeo.2023.106573
- Gu, Y., Wang, Z., Yang, C., Luo, M., Jiang, Y., Luo, X., et al. (2023). Effects of diagenesis on quality of dengying formation deep dolomite reservoir, Central Sichuan Basin, China: insights from petrology, geochemistry and *in situ* U-Pb dating. *Front. Earth Sci.* 10, 1041164. doi:10.3389/feart.2022.1041164
- Gu, Y., Zhou, L., Jiang, Y., Jiang, C., Luo, M., and Zhu, X. (2019). A model of hydrothermal dolomite reservoir facies in Precambrian dolomite, Central Sichuan Basin, SW China and its Geochemical Characteristics. *Acta Geol. Sin. Engl. Ed.* 93 (1), 130–145. doi:10.1111/1755-6724.13770
- Guan, S., Jiang, H., Lu, X., Liang, H., Zhu, G., Cui, J., et al. (2022). Strike-slip fault system and its control on oil and gas accumulation in Central Sichuan Basin. *Acta Pet. Sin.* 43 (11), 1542–1557. doi:10.7623/syxb202211003
- Guo, X., Huang, R., Zhang, D., Li, S., Shen, B., and Liu, T. (2024). Hydrocarbon accumulation and orderly distribution of whole petroleum system in marine carbonate rocks of Sichuan Basin, SW China. *Petroleum Explor. Dev.* 51 (4), 852–869. doi:10.1016/s1876-3804(24)60511-2
- Guo, Z., Zhao, W., Liu, W., Jiang, H., Gu, Z., and Xie, Z. (2025). A comprehensive review of the characteristics, formation, evolution, resource potential, and ultradeep exploration fields of oil-cracking gas in the Ediacaran–Cambrian formations of the Sichuan super gas basin. *Mar. Petroleum Geol.* 173, 107271. doi:10.1016/j.marpetgeo.2024.107271
- Hao, F., Guo, T., Zhu, Y., Cai, X., Zhou, H., and Li, P. (2008). Evidence for multiple stages of oil cracking and thermochemical sulfate reduction in the Puguang gas field, Sichuan Basin, China. *AAPG Bull.* 92 (5), 611–637. doi:10.1306/01210807090
- Harding, T. (1990). Identification of wrench faults using subsurface structural data: criteria and pitfalls. *Am. Assoc. Petroleum Geol. Bull.* 74 (10), 1590–1609. doi:10.1306/0c9b2533-1710-11d7-8645000102c1865d
- He, X., Tang, Q., Wu, G., Li, F., Tian, Z., Luo, W., et al. (2023). Control of strike-slip faults on Sinian carbonate reservoirs in Anyue gas field, Sichuan

by the National Natural Science Foundation of China (Grant No. 42202166), and the National Natural Science Foundation of China (Grant No. 41972165).

Conflict of interest

Authors YC, FL, and LW are employed by PetroChina Southwest Oil and Gas Field Company. Authors JL and XZ are employed by Fores (Chengdu) Technology Co., Ltd.

Generative AI statement

The author(s) declare that no Generative AI was used in the creation of this manuscript.

Publisher's note

All claims expressed in this article are solely those of the authors and do not necessarily represent those of their affiliated organizations, or those of the publisher, the editors and the reviewers. Any product that may be evaluated in this article, or claim that may be made by its manufacturer, is not guaranteed or endorsed by the publisher.

- Basin, SW China. *Petroleum Explor. Dev.* 50 (6), 1282–1294. doi:10.1016/s1876-3804(24)60466-0
- Hips, K., Haas, J., and Györi, O. (2016). Hydrothermal dolomitization of basinal deposits controlled by a synsedimentary fault system in Triassic extensional setting, Hungary. *Int. J. Earth Sci.* 105 (4), 1215–1231. doi:10.1007/s00531-015-1237-4
- Hu, W., Wang, X., Zhu, D., You, D., and Wu, H. (2018). An overview of types and characterization of hot fluids associated with reservoir formation in petroliferous basins. *Energy Explor. Exploitation* 36 (6), 1359–1375. doi:10.1177/0144598718763895
- Hurley, N. F., and Swager, D. R. (1989). Multiscale reservoir heterogeneity in fracture-controlled dolomites, Albion-Scipio and Stoney Point fields, Michigan. *AAPG Bull. (USA)*, 73, 9. doi:10.1306/44B4A72B-170A-11D7-8645000102C1865D
- Jiang, T., Han, J., Wu, G., Yu, H., Su, Z., Xiong, C., et al. (2020). Differences and controlling factors of composite hydrocarbon accumulations in the Tazhong uplift, Tarim Basin, NW China. *Petroleum Explor. Dev.* 47 (2), 229–241. doi:10.1016/s1876-3804(20)60042-8
- Jiang, Y., Tao, Y., Gu, Y., Wang, J., Qiang, Z., Jiang, N., et al. (2016). Hydrothermal dolomitization in Dengying Formation, gaoshiti-moxi area, Sichuan Basin, SW China. *Petroleum Explor. Dev.* 43 (1), 54–64. doi:10.1016/s1876-3804(16)30006-4
- Jiao, F., Yang, Y., Ran, Q., Wu, G., and Liang, H. (2021). Distribution and gas exploration of the strike-slip faults in the central Sichuan Basin. *Nat. Gas. Ind.* 41 (8), 92–101. doi:10.3787/j.issn.1000-0976.2021.08.009
- Koeshidayatullah, A., Corlett, H., Stacey, J., Swart, P. K., Boyce, A., Robertson, H., et al. (2020). Evaluating new fault-controlled hydrothermal dolomitization models: insights from the cambrian dolomite, western Canadian sedimentary basin. *Sedimentology* 67, 2945–2973. doi:10.1111/sed.12729
- Konopásek, J., Janoušek, V., Oyhantçabal, P., Sláma, J., and Ulrich, S. (2018). Did the Circum-Rodinia subduction trigger the Neoproterozoic rifting along the Congo-Kalahari Craton margin? *Int. J. Earth Sci.* 107 (5), 1859–1894. doi:10.1007/s00531-017-1576-4
- Lapponi, F., Bechstäd, T., Boni, M., Banks, D. A., and Schneider, J. (2018). Hydrothermal dolomitization in a complex geodynamic setting (Lower Palaeozoic, northern Spain). *Sedimentology* 61 (2), 411–443. doi:10.1111/sed.12060
- Li, H., Wang, L., Liu, Y., Zeng, T., Zang, D., Li, W., et al. (2021). Hydrothermal activities in the middle permian maokou Formation in eastern Sichuan Basin. *Jouenal Palaeogr. Chin. Ed.* 23 (1), 153–174. doi:10.7605/gdxb.2021.01.011
- Li, K., Gong, B., Zhang, X., Jiang, H., Fan, J., and Tan, Y. (2023). A comparison of hydrothermal events and petroleum migration between Ediacaran and lower Cambrian carbonates, Central Sichuan Basin. *Mar. Petroleum Geol.* 150, 106130. doi:10.1016/j.marpetgeo.2023.106130
- Li, S., Zhao, S., Liu, X., Cao, H., Yu, S., Li, X., et al. (2018). Closure of the proto-tethys ocean and early paleozoic amalgamation of microcontinental blocks in east asia. *Earth-Science Rev.* 186, 37–75. doi:10.1016/j.earscirev.2017.01.011
- Liu, Z., Tan, S., He, X., Wang, D., and Gao, B. (2019). Petrogenesis of mid-Neoproterozoic (ca. 750 Ma) mafic and felsic intrusions in the Ailao Shan-Red River belt: geochemical constraints on the paleogeographic position of the South China block. *Lithosphere* 11 (3), 348–364. doi:10.1130/L1038.1
- Lonnee, J., and Machel, H. G. (2006). Pervasive dolomitization with subsequent hydrothermal alteration in the Clarke Lake gas field, middle devonian slave point formation, British Columbia, Canada. *AAPG Bull.* 90 (11), 1739–1761. doi:10.1306/03060605069
- Luczaj, J. A. (2006). Evidence against the Dorag (Mixing-Zone) model for dolomitization along the Wisconsin arch - a case for hydrothermal diagenesis. *AAPG Bull.* 90 (90), 1719–1738. doi:10.1306/011130605077
- Ma, B., Liang, H., Wu, G., Tang, Q., Tian, W., Zhang, C., et al. (2023). Formation and evolution of the strike-slip faults in the central Sichuan Basin, SW China. *Petroleum Explor. Dev.* 50 (2), 373–387. doi:10.1016/s1876-3804(23)60394-5
- Ma, D., Wang, Z., Duan, S., Gao, J., Jiang, Q., Jiang, H., et al. (2018). Strike-slip faults and their significance for hydrocarbon accumulation in Gaoshiti-Moxi area, Sichuan Basin, SW China. *Petroleum Explor. Dev.* 45 (5), 851–861. doi:10.1016/s1876-3804(18)30088-0
- Ma, K., Wen, L., Zhang, B., Li, Y., Zhong, J., Wang, Y., et al. (2022). Segmented evolution of Deyang-Anyue erosion rift trough in Sichuan Basin and its significance for oil and gas exploration, SW China. *Petroleum Explor. Dev.* 49 (2), 313–326. doi:10.1016/s1876-3804(22)60026-0
- Ma, X., Yang, Y., Wen, L., and Luo, B. (2019). Distribution and exploration direction of medium- and large-sized marine carbonate gas fields in Sichuan Basin, SW China. *Petroleum Explor. Dev.* 46 (1), 1–15. doi:10.1016/s1876-3804(19)30001-1
- Nurkhanuly, U., and Dix, G. R. (2014). Hydrothermal dolomitization of Upper Ordovician limestone, Central-East Canada: fluid flow in a craton-interior wrench-fault system likely driven by distal tectonic tectonism. *J. Geol.* 122 (3), 259–282. doi:10.1086/675666
- Ronchi, P., Masetti, D., Tassan, S., and Camocino, D. (2012). Hydrothermal dolomitization in platform and basin carbonate successions during thrusting: a hydrocarbon reservoir analogue (Mesozoic of Venetian Southern Alps, Italy). *Mar. Petroleum Geol.* 29 (1), 68–89. doi:10.1016/j.marpetgeo.2011.09.004
- Shen, A., Zhao, W., Hu, A., Wang, H., Liang, F., and Wang, Y. (2021). The dating and temperature measurement technologies for carbonate minerals and their application in hydrocarbon accumulation research in the paleo-uplift in central Sichuan Basin, SW China. *Petroleum Explor. Dev.* 48 (3), 555–568. doi:10.1016/s1876-3804(21)60045-9
- Su, A., Chen, H., Feng, Y., Zhao, J., Wang, Z., Hu, M., et al. (2022). *In situ* U-Pb dating and geochemical characterization of multi-stage dolomite cementation in the Ediacaran Dengying Formation, Central Sichuan Basin, China: constraints on diagenetic, hydrothermal and paleo-oil filling events. *Precambrian Res.* 368, 106481. doi:10.1016/j.precamres.2021.106481
- Tian, F., Guo, T., He, D., Gu, Z., Meng, X., Wang, R., et al. (2024). Three-dimensional structural models, evolutions and petroleum geological significances of transtensional faults in the Ziyang area, central Sichuan Basin, SW China. *Petroleum Explor. Dev.* 51 (3), 526–540. doi:10.11698/PED.20230635
- Wang, H., Jiang, Y., Yang, C., Zhang, B., Gu, Y., Luo, X., et al. (2023). Hydrothermal silicification in Ediacaran Dengying Formation fourth member deep dolomite reservoir, Central Sichuan Basin, China: implications for reservoir quality. *Geol. J.* 58 (11), 4257–4270. doi:10.1002/gj.4757
- Wang, Z., Jiang, C., Yang, C., Jiang, Y., and Gu, Y. (2025). Hydrothermal activity and its influence on hydrocarbon accumulation in deep dolomite reservoirs of the Ediacaran Dengying Formation, Sichuan Basin. *Energy Geosci.* 6, 100370. doi:10.1016/j.engeos.2024.100370
- Wei, G., Wang, Z., Li, J., Yang, W., and Xie, Z. (2017). Characteristics of source rocks, resource potential and exploration direction of Sinian-Cambrian in Sichuan Basin, China. *J. Nat. Gas Geoscience* 2 (5), 289–302. doi:10.1016/j.jnggs.2018.02.002
- Wu, G., Zhao, K., Qu, H., Scarselli, N., Zhang, Y., Han, J., et al. (2020). Permeability distribution and scaling in multi-stages carbonate damage zones: insight from strike-slip fault zones in the Tarim Basin, NW China. *Mar. Petroleum Geol.* 114, 104208. doi:10.1016/j.marpetgeo.2019.104208
- Xiao, Y., Wu, G., Lei, Y., and Chen, T. (2017). Analogue modeling of through-going process and development pattern of strike-slip fault zone. *Petroleum Explor. Dev.* 44 (3), 368–376. doi:10.1016/s1876-3804(17)30043-5
- Xie, W., Jiang, H., Ma, S., Wang, Z., Hao, T., Fu, X., et al. (2022). Sedimentary evolution characteristics and favorable exploration directions of DeyangAnyue rift within the Sichuan Basin in late sinian-early cambrian. *Nat. Gas. Geosci.* 33 (8), 1240–1250. doi:10.11764/j.issn.1672-1926.2022.03.012
- Yang, G., Ren, Z., He, F., Zhang, Y., Wang, B., and Qi, K. (2022). Fault-fracture body growth and hydrocarbon enrichment of the Zhenjing area, the southwestern margin of the Ordos Basin. *Oil Gas Geol.* 43 (6), 1382–1383. doi:10.11743/ogg.20220609
- Yang, Z., Zhong, D., Whitaker, F., Lu, Z., Zhang, S., Tang, Z., et al. (2020). Syn-sedimentary hydrothermal dolomites in a lacustrine rift basin: petrographic and geochemical evidence from the lower Cretaceous Erlan Basin, Northern China. *Sedimentology* 67 (1), 305–329. doi:10.1111/sed.12644
- Zhang, Z., Qiao, Y., Dou, S., Li, S., Zhong, Y., Wu, L., et al. (2024). Karst paleogeomorphology and reservoir control model of the 2nd member of Dengying Formation in Penglai gas area, Sichuan Basin, China. *Oil Gas Geol.* 45 (1), 200–214. doi:10.11743/ogg20240114